Arch. Pharm. Chem. Life Sci. 2017, *350*, e1700204

ARCH PHARM
Archiv der Pharmazie

Full Paper

Synthesis, Biological Evaluation, and Molecular Modeling Study of Substituted Benzyl Benzamides as CETP Inhibitors

Reema Abu Khalaf, Dima Sabbah, Eveen Al-Shalabi, Samar Bishtawi, Ghadeer Albadawi, and Ghassan Abu Sheikha

Faculty of Pharmacy, Department of Pharmacy, Al-Zaytoonah University of Jordan, Amman, Jordan

Cardiovascular disease is the most common cause for mortality and morbidity in the developed world; its risk is inversely related to the high-density lipoprotein (HDL) cholesterol levels. Therefore, there is a great interest in developing new cholesteryl ester transfer protein (CETP) inhibitors capable of raising HDL as a novel approach for the prevention of cardiovascular disease. Herein, the synthesis and characterization of ten benzyl benzamides **8a–j** that aim at CETP inhibition was performed. The *in vitro* CETP inhibition bioassay revealed that benzamide **8j** had the best activity, with a percent inhibition of 82.2% at 10 μM concentration and an IC_{50} value of 1.3 μM. The docking study shows that the verified compounds accommodate the binding cleft of CETP and are enclosed by a hydrophobic lining. Furthermore, the scaffold of **8a–j** matches the pharmacophoric points of CETP inhibitors, particularly in its hydrophobic and aromatic functionalities.

Keywords: Atherosclerosis / Benzyl benzamides / CETP inhibitors / Docking / Pharmacophore mapping

Received: June 22, 2017; Revised: October 8, 2017; Accepted: October 10, 2017

DOI 10.1002/ardp.201700204

Additional supporting information may be found in the online version of this article at the publisher's web-site.

Introduction

Cardiovascular disease is the most common cause for mortality and morbidity in the developed world [1]. It encompasses coronary heart disease (CHD), as well as congestive heart failure, stroke, peripheral artery disease, carotid artery disease, and aortoiliac disease [2]. CHD is usually caused by a build-up of fatty deposits on the walls of the arteries around the heart in a process called atherosclerosis, in which low-density lipoprotein cholesterol (LDL-C) plays a major role in its pathophysiology [3].

On the other hand, epidemiological data have clearly demonstrated a strong inverse relationship between high-density lipoprotein cholesterol (HDL-C) levels and the risk of cardiovascular events, which is independent of the LDL-C levels and remains relevant even after the achievement of optimal LDL-C levels [4, 5], and it is thus considered to be an anti-atherogenic lipoprotein [6].

Development of novel therapies is in process to further enhance the atheroprotective properties of HDL [7]. It is believed that reverse cholesterol transport (RCT) is a primary atheroprotective property of HDL and its major protein, apolipoprotein A-I (apoA-I) [8]. So, there is considerable interest in the potential use of pharmacological inhibitors of cholesteryl ester transfer protein (CETP) as a novel approach for cardiovascular disease prevention [9].

Plasma CETP was first described as a high molecular weight glycoprotein [10], consisting of 476 amino acid residues and has a molecular mass of 74 kDa [10, 11]. It belongs to a family of proteins involved in lipid binding [12], stimulating the transfer of cholesteryl ester between lipoproteins [8, 13, 14].

Moreover, the structure of CETP revealed a 60-Å long tunnel structure that demonstrated binding of two neutral lipids, hydrophobic cholesteryl esters in the tunnel, and two phospholipids, phosphatidylcholines, that plug the two distinct openings at each end [15, 16].

Correspondence: Dr. Reema Abu Khalaf, Faculty of Pharmacy, Department of Pharmacy, Al-Zaytoonah University of Jordan, Amman 11180, Jordan.
E-mail: reema.abukhalaf@zuj.edu.jo, rima_abu_khalaf@yahoo.com
Fax: +962 6 4291432

Therefore, CETP may play a dual role in RCT. It may represent an additional route for the delivery of cholesterol to the liver or, if LDL receptors are not fully functional, CETP promotes the accumulation of LDL-C in the plasma, thus favoring the atheroma formation [17]. CETP seems to be anti-atherogenic. However, when it is altered, either by receptor malfunction or defective ligands, CETP becomes pro-atherogenic [18].

Early discovered CETP inhibitors (Fig. 1) are torcetrapib, dalcetrapib, anacetrapib, and evacetrapib [19]. A randomized evaluation of the effects of anacetrapib shows that anacetrapib appears to be safe, well-tolerated, and delivers a substantial increases in HDL-C and reductions in LDL-C as monotherapy and when combined with a statin [20, 21].

Although CETP acts as an antiatherogenic protein in certain human mutant studies, most clinical and experimental evidences support that CETP is atherogenic in nature [22, 23].The role of CETP-mediated lipid transfer in the development of atherosclerosis and CETP inhibition as a potential strategy for prevention of atherosclerosis have been controversial [24].

Our research group identified different potential CETP inhibitors including benzenesulfonamides and toluene-4-sulfonic acid esters [5], benzylamino-methanones [11], fluorinated benzamides [16], benzylideneamino-methanones [23], and chlorobenzyl benzamides [25].

In order to optimize the activity of our previously discovered hit compounds [25], variable substituents at the *meta* and *para* positions were utilized (*p*-OCH_3, *p*-CH_3, *m*-Br, *m*-F, and *p*-F) followed by *in vitro* CETP inhibition bioassay.

Results and discussion

Chemistry

A series of benzyl benzamides **8a–j** were synthesized as shown in Scheme 1. The synthesis started with the activation of the

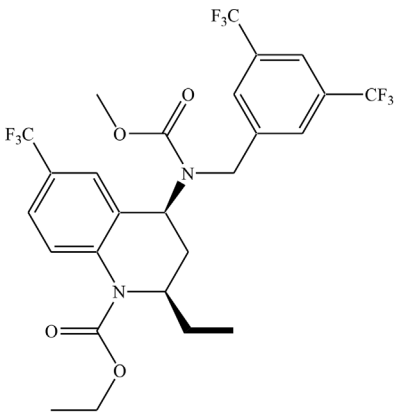

Torcetrapib

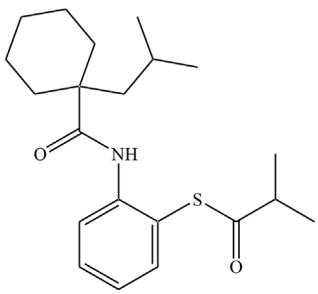

Dalcetrapib

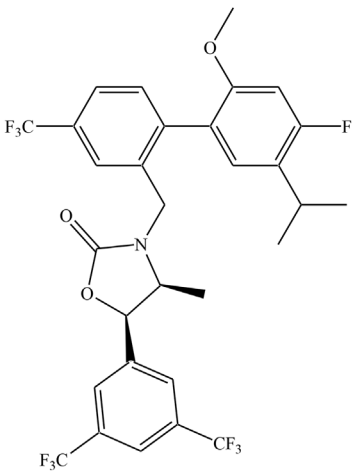

Anacetrapib

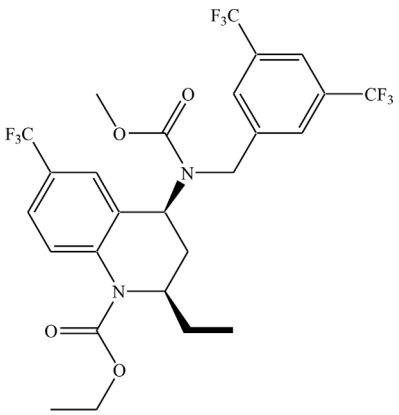

Evacetrapib

Figure 1. Chemical structures CETP inhibitors.

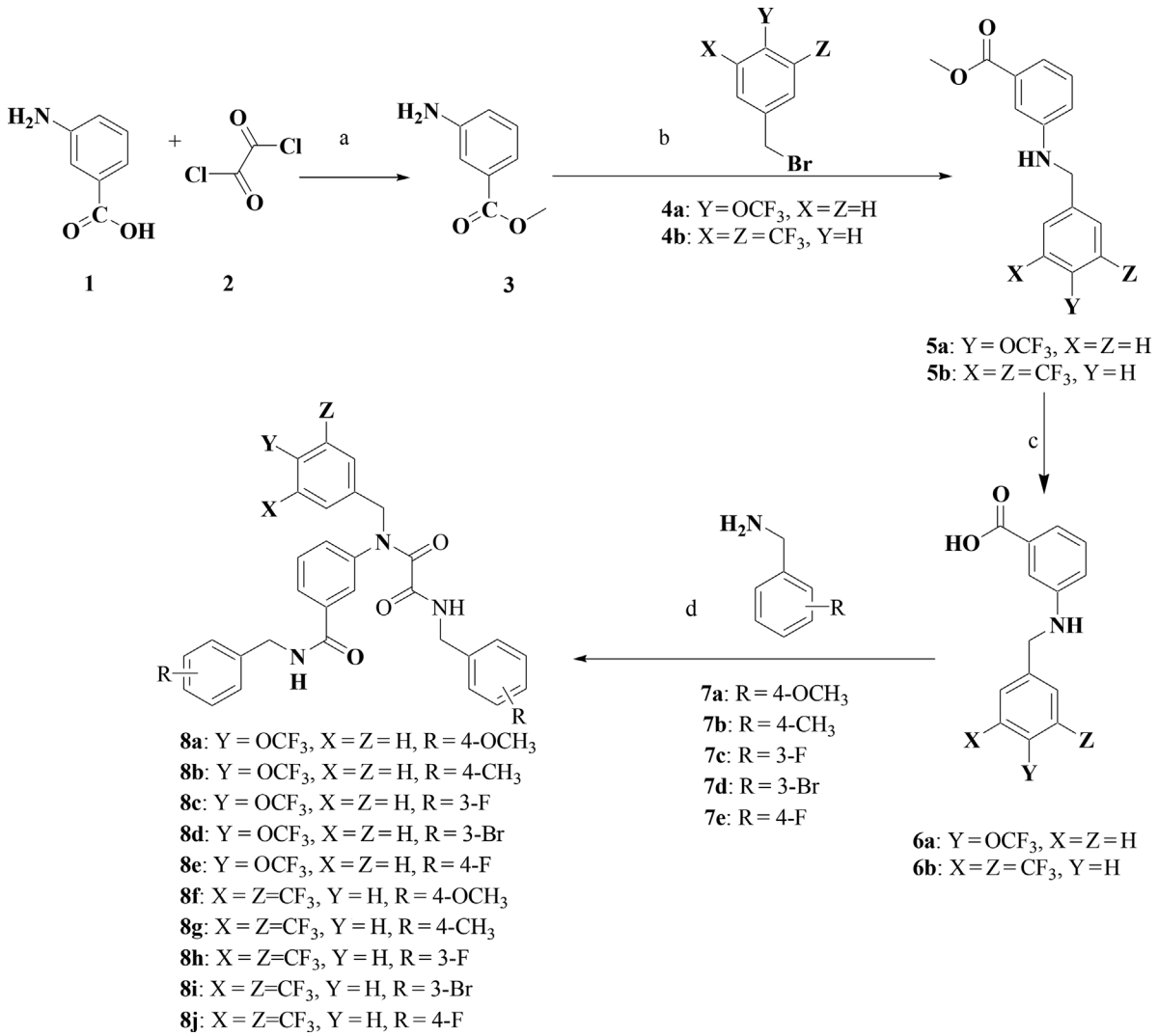

Scheme 1. Synthesis of benzyl benzamide derivatives **8a–j**. Reagents and conditions: (a) CH_3OH/reflux (60–70°C), 24 h; (b) DCM, TEA, RT, 5 days; (c) (1) 1 M NaOH (100°C), overnight, (2) 1 M HCl; (d) $(COCl)_2$, TEA, DCM, RT, 5 days.

carboxylic acid moiety of 3-aminobenzoic acid (**1**) using oxalyl chloride (**2**) in the presence of methanol to produce the corresponding methyl ester protecting group (**3**). Next, the amine nitrogen of 3-amino benzoic acid methyl ester (**3**) attacked the partially positive methylene group of the benzyl bromide (**4a,b**) in the presence of DCM as a solvent to produce substituted 3-benzylaminobenzoic acid methyl ester intermediates (**5a,b**). Triethylamine was used as an acid scavenger.

It was found that **5a** (44% yield) was produced in higher yield than **5b** (28%). Afterward, deprotection of the carboxylic acid group of 3-aminobenzoic acid methyl ester intermediates (**5a,b**) was carried out by alkaline hydrolysis using 1 M NaOH under reflux followed by neutralization with 1 M HCl. Again, activation of the carboxylic acid moiety of 3-benzylamino benzoic acid intermediates (**6a,b**) was performed using oxalyl chloride (**2**) to produce the corresponding acyl chloride derivatives in the presence of TEA and DCM. Additionally, oxalyl chloride reacted with the amine moiety of 3-benzylamino benzoic acid intermediates (**6a,b**). Subsequently, amide formation was attained by the nucleophilic attack of the amine moiety of benzylamine (**7a–e**) on the partially positive carbonyl carbon of the previously produced benzoyl chloride and acyl chloride to get the targeted benzyl benzamide derivatives **8a–j**.

The best yield was obtained upon reacting intermediate **6a** with 4-methoxy benzylamine (**7a**) to produce **8a** in 53% yield.

In vitro CETP inhibition bioassay

The results of CETP inhibition bioassay, presented in Table 1, demonstrate that all the synthesized benzamides **8a–j** have appreciable CETP inhibitory activity with the compound **8j** exhibiting promising activity against CETP with a percent inhibition of 82.1% at 10 μM concentration and an IC_{50} of 1.3 μM.

Structure–activity relationship study of the synthesized compounds **8a–j** reveals that (Scheme 1 and Table 1) the presence of *para* trifluoromethoxy group (as in compounds **8a** and **8b**) gives greater inhibitory activity than the two *meta* trifluoromethyl groups (as in compounds **8f** and **8g**) when the structure is substituted with a lipophilic and electron donating R groups, i.e. OCH_3 and CH_3. Conversely, existence of lipophilic and electron withdrawing R groups such as F and Br enhances the inhibitory activity more in the presence of the two *meta* trifluoromethyl groups (as in compounds **8h–j**).

Furthermore, it looks that the position of the fluorine substituent whether at the *meta* or *para* position has greater influence on the CETP inhibitory activity of the synthesized compound when the structure is substituted with 3,5-ditrifluoromethyl moieties (as in compounds **8h** and **8j**) rather than 4-trifluoromethoxy group (as in compounds **8c** and **8e**). Moreover, comparing the activities of the synthesized compounds having *m*-F groups (as in compounds **8c** and **8h**) with those containing *m*-Br moieties (as in compounds **8d** and **8i**) shows that *m*-F derivatives are more active than *m*-Br ones.

Docking studies

In order to identify the structural basis of binding of the co-crystallized ligand (ORP: torcetrapib) and **8a–j** in CETP (PDB ID: 4EWS), we carried out docking studies employing Glide [26, 27] docking approach against 4EWS. The Glide docking data for **8a–j** and ORP show that these compounds bind to the active site of 4EWS. Indeed, Fig. 2 demonstrates that the docked pose of **8i** superposed the conformation of ORP (torcetrapib).

Of note is the dominance of hydrophobic interaction between the bound ligands and the backbones of the key binding residues of 4EWS (Table 2; Figs. 3 and 4; Supporting Information Figs. S1 and S2).

The docking scores demonstrate the high binding affinity of this series toward 4EWS. The more negative the docking score, the higher is the binding affinity and consequently the better is the binder. Distinctly, a 2 kcal/mol difference in the docking score of the co-crystallized ligand (ORP: torcetrapib) and **8g**,**h** infers that this scaffold might be a promising core structure for CETP inhibition. Figure 5 shows that there is a positive correlation between the % inhibition and Glide docking scores against CETP ($R^2 = 0.81$).

The *in vitro* biological data elucidates that compounds (**8a–e**) tailored with *p*-OCF_3 moiety exerted promising CETP inhibition; particularly **8a–c** and **8e**. Results suggests that hydrophobic and/or H-bond acceptor cleft accommodates the *p*-OCH_3 motifs in **8a**. In addition, the inhibitory activity of **8b**

Table 1. ***In vitro*** **bioactivities of synthesized benzyl benzamides 8a–j.**

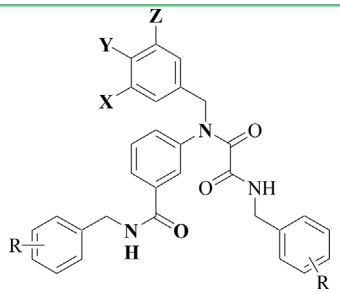

Compound	Y	X	Z	R	% Inhibition	IC_{50} (μM)
8a	OCF_3	H	H	4-OCH_3	65.8[a)]	3.7 ($R^2 = 0.98$)
8b	OCF_3	H	H	4-CH_3	62.1[a)]	4.4 ($R^2 = 0.96$)
8c	OCF_3	H	H	3-F	50.0[a)]	–
8d	OCF_3	H	H	3-Br	21.9[a)]	–
8e	OCF_3	H	H	4-F	51.1[a)]	–
8f	H	CF_3	CF_3	4-OCH_3	54.8[a)]	–
8g	H	CF_3	CF_3	4-CH_3	37.5[a)]	–
8h	H	CF_3	CF_3	3-F	59.6[a)]	–
8i	H	CF_3	CF_3	3-Br	28.5[a)]	–
8j	H	CF_3	CF_3	4-F	82.1[a)]	1.3 ($R^2 = 0.99$)
Torcetrapib	–	–	–	–	82.2[b)]	0.04

[a)] Tested at 10 μM concentration. [b)] Tested at 0.08 μM concentration.

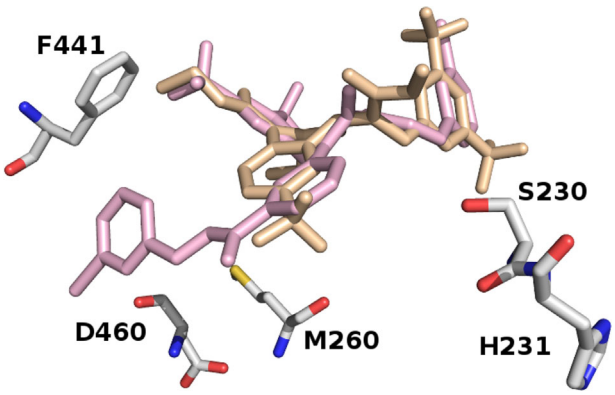

Figure 2. Superposition of the Glide docked pose of **8i** (represented in pink color) and the cocrystallized ligand (gold color). H atoms and some of key binding residues are hidden for clarity purpose. Picture made by PYMOL.

confirms that hydrophobic interaction is favored on *p*-position. Remarkably, the % inhibition of **8e** endorses that hydrophobic interaction is essential on *p*-position to elicit a biological activity. It is worth noting that **8c** exerted comparable inhibitory activity to that of **8e**; such finding recommends small hydrophobic and/or H-bond acceptor motifs on *m*-position. Actually, the activity of **8d** implies that a tight binding cleft surrounds the *m*-position and hinders the proper accommodation of −Br in **8d**.

Comparable inhibitory activity was noticed for analogues bearing two *m*-CF_3 groups instead of *p*-OCF_3 (**8f–j**). Surprisingly, the inhibitory activity of **8j** matches that of the reference inhibitor (torcetrapib). Result suggests that the two *m*-CF_3 groups occupy part of the binding site thus favors small moiety such as *p*-F in **8j**. Accordingly, the activity of **8f** confirms that a steric effect hinders the orientation of *p*-OCH_3 motifs in the binding domain and therefore clarifies its moderate activity. Additionally, incorporating a fluoro moiety on *m*-position (**8h**) implies that small binding cleft encloses the *m*-position and thus explains the weak inhibitory activity of **8i**. The weak activity of **8g** confirms the steric hindrance effect and recommends attaching a small motif on *p*-position. Moreover, the difference between the activity of **8f** and **8g** is due to oxygen atom that might direct the methyl deeper in the binding domain. Also, the O-atom provides a water accessible surface area that facilitates the interaction between the polar key binding residues and the backbone of **8f**. Altogether, *p*- and *m*-substituents are favored for small motif provided the core structure is tailored with two *m*-CF_3 groups. On the other hand, analogues bearing *p*-OCF_3 favored hydrophobic and/or H-bond acceptor on *p*- and *m*-positions provided small size attachment on *m*-position whereas the *p*-position shows no restriction on the motif's size and favors *p*-OCH_3 (**8a**), *p*-CH_3 (**8b**), and *p*-F (**8e**). Comparing the activity of analogues incorporating *p*-OCF_3 with those tailored with two *m*-CF_3 recommends the two *m*-CF_3 group and this accords with the hydrophobic interaction that guides ligand/protein complex formation.

Table 2. The Glide docking scores (Kcal/mol) of the verified compounds.

Compound	Glide docking scores (kcal/mol)	H-Bond
8a	−11.26	H232
8b	−12.29	NA
8c	−11.13	NA
8d	−12.32	R201
8e	−11.24	NA
8f	−12.35	NA
8g	−12.52	NA
8h	−12.56	NA
8i	−12.26	NA
8j	−11.90	NA
Torcetrapib (ORP)	−10.57	NA

NA: not available.

Pharmacophore mapping

In order to explore the backbones of **8a–j** and their attachments, we screened them against CETP inhibitors pharmacophore model [16]. We found that **8a–j** match the CETP inhibitors fingerprint (Figs. 6 and 7; Supporting Information Figs. S3 and S4) and this explains the affinity of **8a–j** toward CETP active domain. Moreover, **8a–j** accommodate CETP active binding domain thus explaining their inhibitory activity.

Conclusion

Successful synthesis, characterization, biological evaluation, and modeling studies of ten new benzamides were carried out. Synthesized compound **8j** was found to present a worthy lead compound for CETP inhibitors with an IC_{50} of 1.3 μM. Benzyl benzamides can serve as a promising new class of CETP inhibitors that can be further structurally optimized to improve CETP inhibitory activity and to enhance understanding of the structure–activity relationship.

Experimental

Chemistry

General

All chemicals, reagents, and solvents were of analytical grade and used directly without extra purification. Chemicals and solvents were purchased from the corresponding companies (Alfa Aesar, Acros Organics, Sigma–Aldrich, Fluka, SD Fine Chem Limited, Tedia and Fisher Scientific).

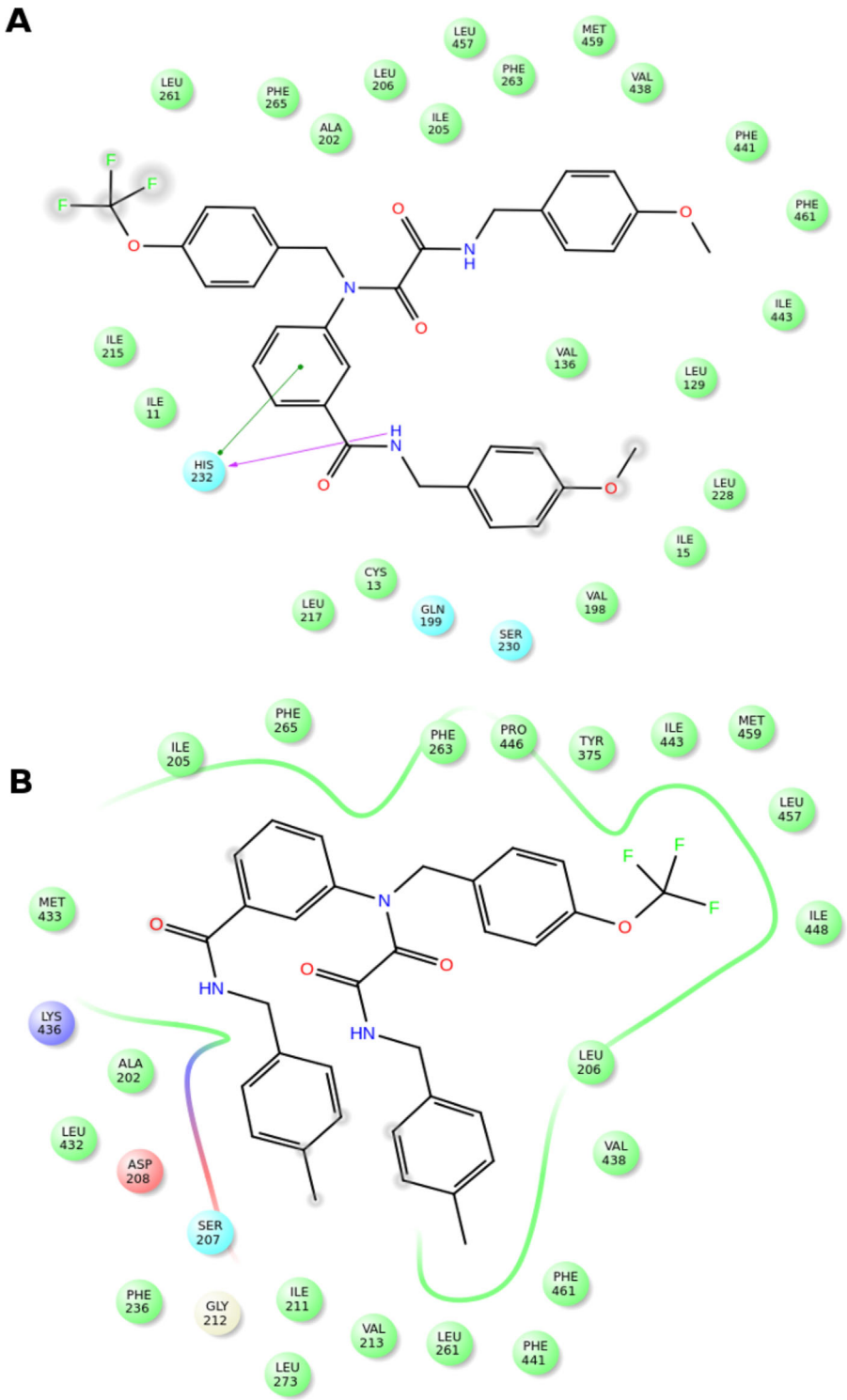

Figure 3. The ligand/protein complex of (A) **8a** and (B) **8b**. The hydrophobic lining is represented in green color. Picture made by MAESTRO [28].

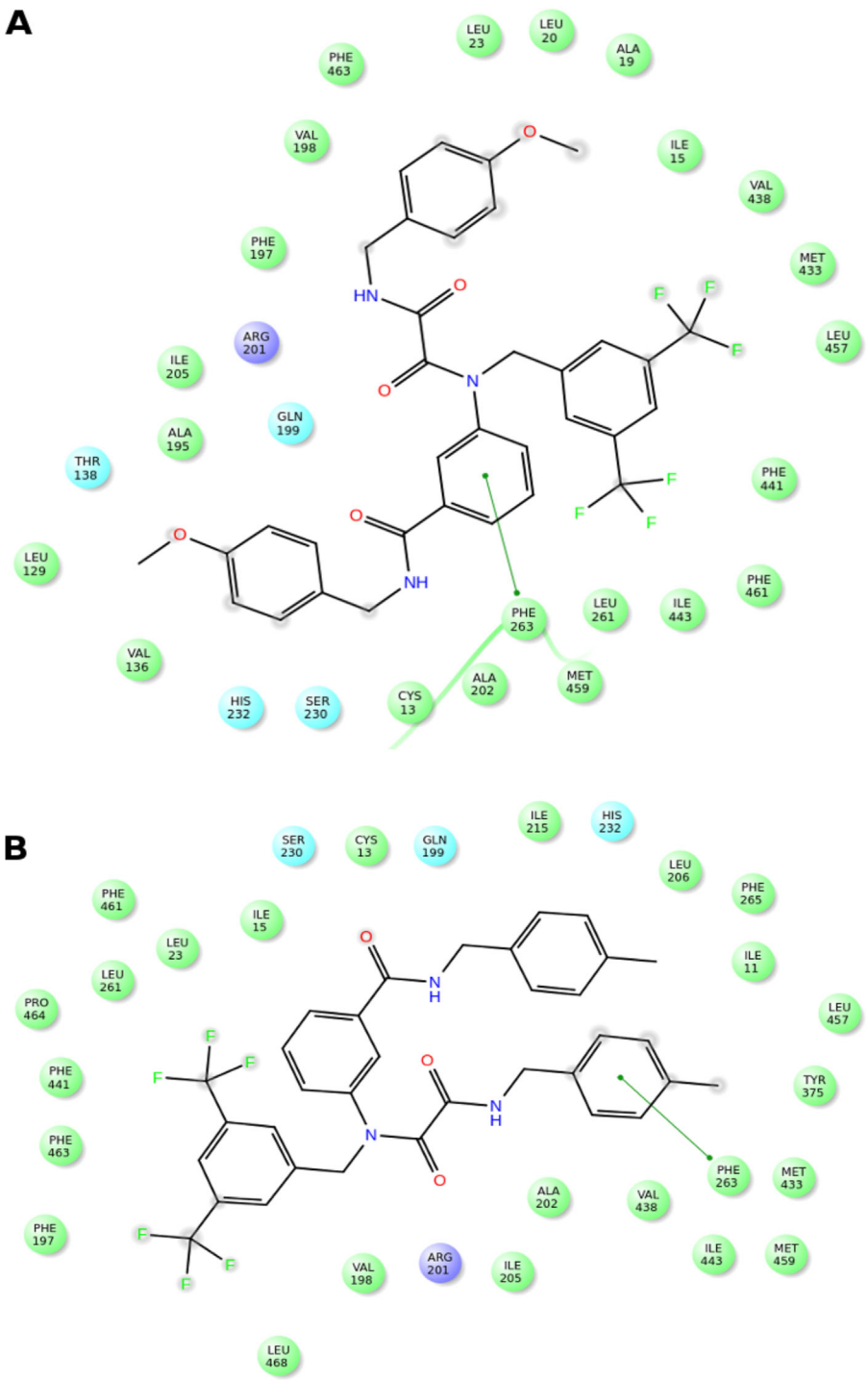

Figure 4. The ligand/protein complex of (A) **8f** and (B) **8g**. The hydrophobic lining is represented in green color. Picture made by MAESTRO [28].

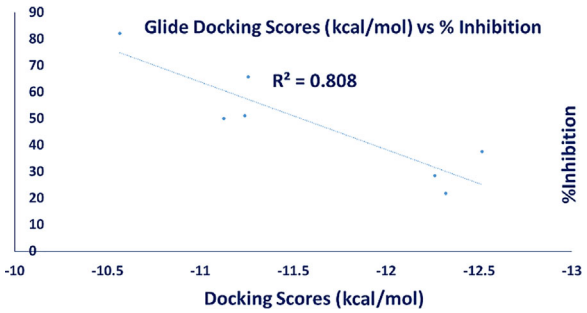

Figure 5. The correlation between % inhibition of CETP and Glide docking scores for the verified compounds. Outliers are deleted for clarity purpose.

Melting points were measured using Gallenkamp melting point apparatus and are uncorrected. Infrared (IR) spectra were recorded using Shimadzu IR Affinity1 FTIR spectrophotometer. All samples were prepared with potassium bromide and pressed into a disc. ^{1}H NMR and ^{13}C NMR spectra were measured on Bruker Avance DPX 500, 400 and Bruker 300 MHz-Avance III spectrometers. Chemical shifts are given in δ (ppm) using TMS as internal reference; the samples were dissolved in $CDCl_3$ or DMSO-d_6. High resolution mass spectrometry (HR-MS) was performed using LC Mass Bruker Apex-IV mass spectrometer utilizing an electrospray interface. AFLX800TBI microplate fluorimeter was used in the *in vitro* bioassay (BioTek Instruments, Winooski, VT, USA).

Thin-layer chromatography (TLC) was performed on 20 × 20 cm with layer thickness of 0.2 mm aluminum cards pre-coated with fluorescent silica gel GF254 DC-Alufolien-Kieselgel (Fluka Analytical, Germany), and visualized by UV light indicator (at 254 and/or 360 nm). Commercially available CETP inhibition drug screening kit was used (BioVision, Linda Vista Avenue, USA).

The InChI codes of the investigated compounds together with some biological activity data are provided as Supporting Information.

*General procedure for the synthesis of methyl benzoates intermediates (**5a,b**) [25]*

3-Aminobenzoic acid (**1**, 2.0 g, 14.58 mmol) was dissolved in methanol (20 mL) and cooled in the ice bath. The solution was treated with oxalyl chloride (**2**, 2.5 mL, 29 mmol) stirred at room temperature for 20–30 min, and refluxed for 24 h at 60–70°C. The reaction mixture was then evaporated and neutralized by 3 M potassium carbonate. Four times extraction by chloroform (4 × 20 mL) was applied. The organic layer was dried with sodium sulfate anhydrous followed by evaporation to get 2.07 g of pure 3-aminobenzoic acid methyl ester (**3**). Next, 3-aminobenzoic acid methyl ester (**3**, 2.0 g, 13.2 mmol) was dissolved in (20 mL) dichloromethane.

*Methyl 3-(4-(trifluoromethoxy)benzylamino)benzoate (**5a**) [25]*

Addition of 1-(bromomethyl)-4-(trifluoromethoxy) benzene (**4a**, 4.2 mL, 26.4 mmol), and triethylamine (9.2 mL, 66 mmol) to the solution of **3** was done. The mixture was left under stirring at room temperature for 5 days, then the mixture was evaporated. Column chromatography was carried out using cyclohexane/ethyl acetate (9:1) as eluent to afford **5a** as off white powder (2.18 g, 44%); m.p. 85–86°C; R_f = 0.46 (cyclohexane/ethyl acetate, 9:1); ^{1}H NMR (300 MHz, $CDCl_3$): δ 3.84 (s, 2H, NHCH_2), 4.63 (s, 3H, OCH_3), 6.83 (dd, J = 4, 15 Hz, 1H, Ar-*H*), 7.20 (d, J = 12 Hz, 2H, Ar-*H*), 7.22–7.25 (m, 4H, Ar-*H*), 7.40 (d, J = 12 Hz, 1H, Ar-*H*), 7.44 ppm (s, 1H, N*H*CH$_2$); ^{13}C NMR (75 MHz, $CDCl_3$): δ 53.6, 59.6, 113.4, 117.1, 118.7, 121.4, 128.1, 129.5, 136.5, 150.0, 168.0 ppm; IR (KBr): 3480, 3225, 2986, 1713, 1620, 1458, 1404, 1303, 1250 cm^{-1}.

*Methyl 3-(3,5-bis(trifluoromethyl)benzyl)benzylamino)-benzoate (**5b**) [25]*

Addition of 1-(bromomethyl)-3,5-bis(trifluoromethyl)benzene (**4b**, 4.6 mL, 25 mmol), and triethylamine (8.76 mL, 62 mmol) to the solution of **3** was done. The mixture was left under stirring at room temperature for 7 days then the mixture was evaporated. Column chromatography was carried out using cyclohexane/ethyl acetate (8.5:1.5) as eluent to afford **5b** as yellow powder (1.34 g, 28%); m.p. 109–110°C; R_f = 0.66 (chloroform, 10); ^{1}H NMR (300 MHz, $CDCl_3$): δ 3.86 (s, 3H, OCH_3), 4.33 (t, J = 6 Hz, 1H, N*H*CH$_2$), 4.49 (d, J = 6 Hz, 2H, HNCH_2), 6.73 (dd, J = 3, 9 Hz, 1H, Ar-*H*), 7.19 (t, J = 9 Hz, 1H, Ar-*H*), 7.29 (d, J = 3 Hz, 1H, Ar-*H*), 7.40 (d, J = 9 Hz, 1H, Ar-*H*), 7.82 ppm (d, J = 12 Hz, 3H, Ar-*H*); ^{13}C NMR (75 MHz, $CDCl_3$): δ 47.5, 52.1, 113.7, 117.4, 119.7, 121.4, 121.5, 121.6, 127.4, 129.5, 131.3, 142.0, 147.3, 168.0 ppm; IR (KBr): 3402, 2955, 1713, 1605, 1512, 1443, 1381, 1297 cm^{-1}.

*General procedure for the synthesis of the targeted compounds (**8a–e**)*

The intermediate methyl 3-(4-(trifluoromethoxy)benzylamino)benzoate (**5a**) was dissolved in 1 M sodium hydroxide (5 mL) and refluxed overnight at 100°C, then the reaction mixture was neutralized with 1 M hydrochloric acid and extracted three times using chloroform (3 × 20 mL). The organic layer was dried using anhydrous sodium sulfate and evaporated. Subsequently, the intermediate 3-(4-(trifluoromethoxy)benzylamino)benzoic acid (**6a**, 0.31 g, 1.0 mmol) was dissolved in 10 mL dichloromethane and oxalyl chloride (**2**, 0.17 mL, 2.0 mmol) was added. The reaction was left under stirring for 5 days at 50–60°C. Later the reaction mixture was evaporated.

*3-{(4-(Trifluoromethoxybenzyl)-[3-(4-trifluoromethoxybenzylamino)benzoyl]amino}-N-(4-methoxyobenzyl)benzamide (**8a**)*

4-Methoxy benzylamine (**7a**, 0.39 mL, 3.0 mmol) was added together with 5 mL of triethylamine and stirred at room temperature for 5 days. Then the crude product was purified

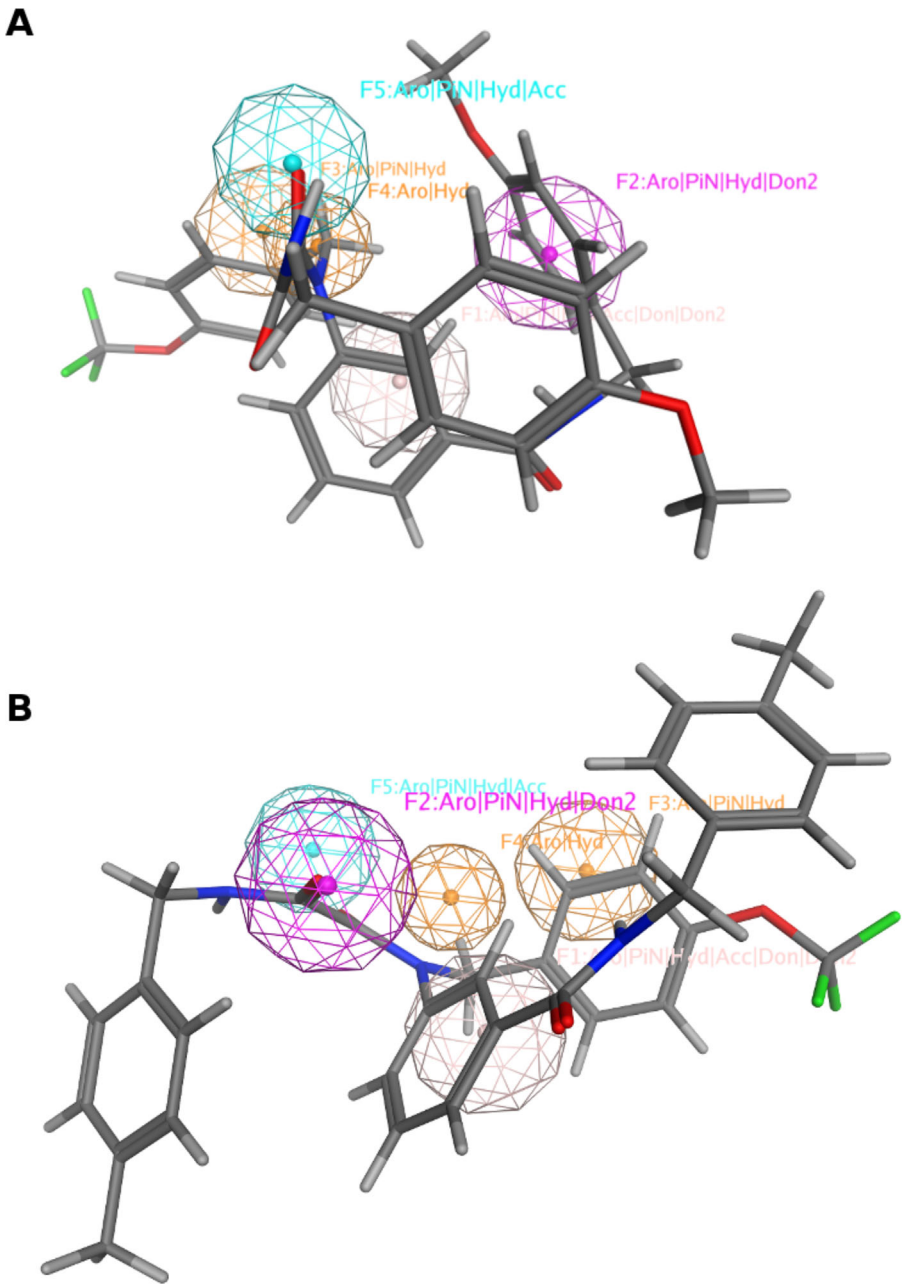

Figure 6. CETP inhibitor pharmacophore model with (A) **8a** and (B) **8b**. Aro stands for aromatic rings; Acc for H-bond acceptor; Don for H-bond donor; Cat for cationic group, PiN for π-ring; and Hyd for hydrophobic groups. Picture made by MOE [29].

by column chromatography using chloroform/Methanol (99:1) as eluent to afford **8a** as white powder (53%); m.p. 130.5–131.5°C; $R_f = 0.90$ ($CHCl_3$/MeOH, 90:10); ^{1}H NMR (500 MHz, DMSO-d_6): δ 3.71 (s, 3H, OCH_3), 3.72 (s, 3H, OCH_3), 4.07 (d, $J = 5.85$ Hz, 2H, CH_2), 4.41 (d, $J = 5.80$ Hz, 2H, CH_2), 5.02 (s, 2H, CH_2), 6.77 (d, $J = 8.55$ Hz, 2H, Ar-*H*), 6.82 (d, $J = 8.50$ Hz, 2H, Ar-*H*), 6.88 (d, $J = 8.55$ Hz, 4H, Ar-*H*), 7.24 (d, $J = 8.55$ Hz, 4H, Ar-*H*), 7.27–7.31 (m, 1H, Ar-*H*), 7.36–7.39 (m, 2H, Ar-*H*), 7.82–7.85 (m, 1H, Ar-*H*), 8.98 (t, $J = 5.85$ Hz, 1H, CON*H*), 9.14 (t, $J = 5.80$ Hz, 1H, CON*H*) ppm; ^{13}C NMR (125 MHz, DMSO-d_6): δ 41.4 (1C), 42.6 (1C), 50.9 (1C), 55.2 (2C), 114.1 (2C), 114.2 (4C), 121.4 (2C), 126.6 (1C), 126.8 (1C), 128.8 (2C), 129.1 (4C), 130.3 (2C), 131.9 (1C), 135.9 (1C), 136.4 (1C), 140.9 (1C), 148.0 (1C), 158.7 (2C), 163.3 (1C), 165.4 (1C),

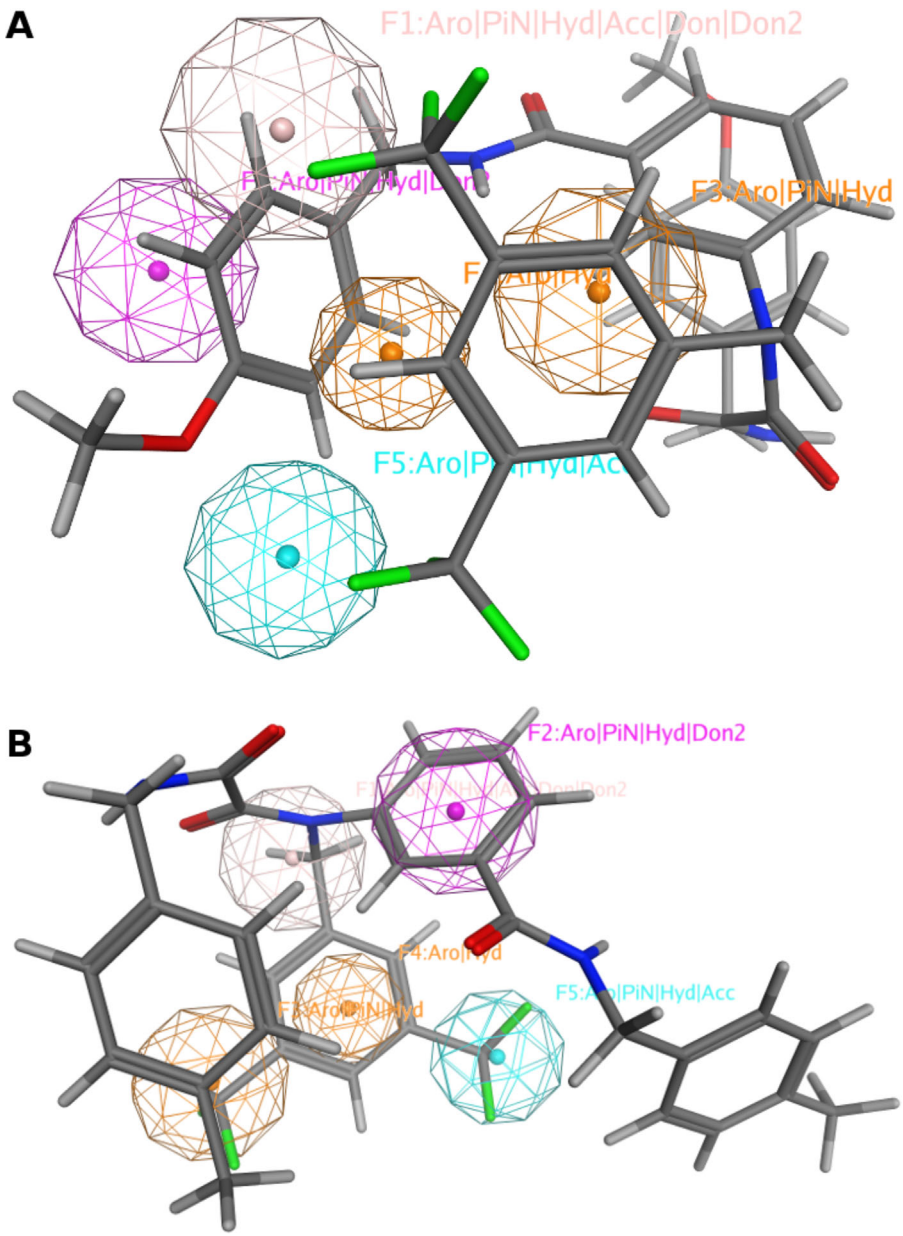

Figure 7. CETP inhibitor pharmacophore model with (A) **8f** and (B) **8g**. Aro stands for aromatic rings; Acc for H-bond acceptor; Don for H-bond donor; Cat for cationic group; PiN for π-ring; and Hyd for hydrophobic groups. Picture made by MOE [29].

165.5 (1C) ppm; IR (KBr): 3318, 3094, 2963, 1651, 1512, 1443, 1319, 1258 cm^{-1}; HR-MS (ESI, negative mode) *m/z* $[M-1]^+$ 620.20074 ($C_{33}H_{29}F_3N_3O_6$ requires 620.20867).

*3-{(4-(Trifluoromethoxybenzyl)-[3-(4-trifluoromethoxybenzylamino)benzoyl]amino}-N-(4-methylbenzyl)benzamide (**8b**)*

4-Methyl benzylamine (**7b**, 0.38 mL, 3.0 mmol) was added together with 5 mL of triethylamine and stirred at room temperature for 5 days. Then the crude product was purified by column chromatography using cyclohexane/ethyl acetate (65:35) as eluent to afford **8b** as white powder (46%); m.p. 162–163°C; $R_f = 0.93$ ($CHCl_3$/MeOH, 90:10); ^{1}H NMR (500 MHz, DMSO-d_6): δ 2.23 (s, 3H, CH_3), 2.28 (s, 3H, CH_3), 4.10 (d, $J = 5.85$ Hz, 2H, CH_2), 4.44 (d, $J = 5.70$ Hz, 2H, CH_2), 5.02 (s, 2H, CH_2), 6.79 (d, $J = 7.80$ Hz, 2H, Ar-*H*), 6.83 (d, $J = 7.75$ Hz, 2H, Ar-*H*), 6.88 (d, $J = 8.55$ Hz, 4H, Ar-*H*), 7.14 (d, $J = 7.90$ Hz, 2H, Ar-*H*), 7.20 (d, $J = 7.85$ Hz, 2H, Ar-*H*), 7.29–7.30 (m, 1H, Ar-*H*),

7.36–7.39 (m, 2H, Ar-*H*), 7.83–7.86 (m, 1H, Ar-*H*), 9.00 (t, $J = 5.85$ Hz, 1H, CON*H*), 9.17 (t, $J = 5.70$ Hz, 1H, CON*H*) ppm; ^{13}C NMR (125 MHz, DMSO-d_6): δ 21.1 (1C), 26.8 (1C), 41.7 (1C), 42.9 (1C), 51.0 (1C), 121.4 (1C), 121.5 (1C) 126.7 (1C), 126.8 (1C), 127.4 (2C), 127.7 (4C), 129.2 (2C), 129.3 (4C), 130.3 (2C), 135.5 (1C), 135.8 (1C), 136.3 (2C), 136.9 (1C), 140.9 (1C), 148.0 (1C), 163.4 (1C), 165.5 (2C) ppm; IR (KBr): 3356, 3071, 2924, 2862, 1659, 1543, 1435, 1397, 1258 cm^{-1}; HR-MS (ESI, negative mode) *m/z* $[M-1]^+$ 588.21019 ($C_{33}H_{29}F_3N_3O_4$ requires 588.21884).

*3-{(4-(Trifluoromethoxybenzyl)-[3-(4-trifluoromethoxybenzylamino)benzoyl]amino}-N-(3-fluorobenzyl)benzamide (**8c**)*

3-Fluorobenzylamine (**7c**, 0.34 mL, 3.0 mmol) was added together with 5 mL of triethylamine and stirred at room temperature for 5 days. Then the crude product was purified by column chromatography using chloroform/acetone (90:10) as eluent to afford **8c** as ivory viscous liquid (29%); $R_f = 0.60$ ($CHCl_3$/ethylacetate, 70:30); ^{1}H NMR (500 MHz, $CDCl_3$): δ 4.27 (d, $J = 5.9$ Hz, 2H, CH_2), 4.56 (d, $J = 6.0$ Hz, 2H, CH_2), 4.94 (s, 2H, CH_2), 6.40–6.53 (m, 1H, Ar-*H*), 6.81 (d, $J = 9.25$ Hz, 1H, Ar-*H*), 6.92 (m, 2H, Ar-*H*), 6.95–7.00 (m, 2H, Ar-*H*), 7.01–7.07 (m, 1H, Ar-*H*), 7.08 (d, $J = 8.3$ Hz, 2H, Ar-*H*), 7.21 (d, $J = 8.1$ Hz, 2H, Ar-*H*), 7.24 (s, 1H, Ar-*H*), 7.26–7.28 (m, 1H, Ar-*H*), 7.33 (m, 1H, Ar-*H*), 7.44–7.52 (m, 1H, Ar-*H*), 7.55 (s, 1H, Ar-*H*), 8.55 (t, $J = 5.9$ Hz, 1H, CON*H*), 8.75 (t, $J = 6.0$ Hz, 1H, CON*H*) ppm; ^{13}C NMR (125 MHz, $CDCl_3$): δ 43.6 (2C), 54.0 (1C), 114.4 (1C), 114.5 (1C), 114.7 (2C), 114.8 (2C), 121.0 (2C), 123.2 (1C), 123.4 (1C), 125.8 (1C), 126.2 (1C), 129.4 (1C), 130.2 (1C), 130.3 (1C), 130.4 (2C), 134.3 (1C), 135.5 (1C), 139.5 (1C), 140.5 (1C), 142.1 (1C), 150.0 (1C), 160.0 (1C), 161.9 (1C), 162.0 (1C), 164.0 (1C), 166.2 (1C) ppm; IR (KBr): 3364, 3071, 2963, 2855, 1667, 1589, 1543, 1451, 1250 cm^{-1}.

*3-{(4-(Trifluoromethoxybenzyl)-[3-(4-trifluoromethoxybenzylamino)benzoyl]amino}-N-(3-bromobenzyl)benzamide (**8d**)*

3-Bromobenzylamine (**7d**, 0.38 mL, 3.0 mmol) was added together with 5 mL of triethylamine and stirred at room temperature for 5 days. Then the crude product was purified by column chromatography using chloroform/methanol (95:5) as eluent to afford **8d** as yellow viscous liquid (20%); $R_f = 0.70$ ($CHCl_3$/MeOH, 98:2); ^{1}H NMR (300 MHz, $CDCl_3$): δ 4.27 (d, $J = 6.0$ Hz, 2H, CH_2), 4.57 (d, $J = 6.0$ Hz, 2H, CH_2), 4.91 (s, 2H, CH_2), 6.24–6.51 (m, 1H, Ar-*H*), 7.13 (d, $J = 6.0$ Hz, 2H, Ar-*H*), 7.20 (s, 2H, Ar-*H*), 7.24 (s, 1H, Ar-*H*), 7.29–7.43 (m, 6H, Ar-*H*), 7.45–7.51 (m, 2H, Ar-*H*), 7.55 (s, 1H, Ar-*H*), 7.65 (d, $J = 6.0$ Hz, 1H, Ar-*H*), 8.55 (t, $J = 6.0$ Hz, 1H, CON*H*), 8.63 (t, $J = 6.0$ Hz, 1H, CON*H*) ppm; ^{13}C NMR (75 MHz, $CDCl_3$): δ 42.8 (1C), 43.6 (1C), 54.2 (1C), 121.1 (2C), 125.8 (1C), 126.2 (1C), 126.4 (1C), 126.6 (1C), 129.5 (1C), 130.3 (1C), 130.4 (2C), 130.5 (2C), 130.8 (2C), 130.9 (2C), 131.0 (2C), 134.2 (1C), 139.1 (1C), 140.0 (1C), 142.1 (1C), 144.5 (1C), 149.3 (1C), 152.5 (1C), 160.0 (1C), 162.1 (1C), 166.5 (1C) ppm; IR (KBr): 3325, 3071, 2963, 2855, 1651, 1543, 1427, 1265 cm^{-1}.

*3-{(4-(Trifluoromethoxybenzyl)-[3-(4-trifluoromethoxybenzylamino)benzoyl]amino}-N-(4-fluorobenzyl)benzamide (**8e**)*

4-Fluorobenzylamine (**7e**, 0.34 mL, 3.0 mmol) was added together with 5 mL of triethylamine and stirred at room temperature for 5 days. Then the crude product was purified by column chromatography using cyclohexane/ethyl acetate (60:40) as eluent to afford **8e** as off-white powder (46.3%); m.p. 140.5–141.5°C; $R_f = 0.62$ ($CHCl_3$/MeOH, 98:2); ^{1}H NMR (400 MHz, DMSO-d_6): δ 4.01 (d, $J = 4.0$ Hz, 2H, CH_2), 4.45 (d, $J = 4.0$ Hz, 2H, CH_2), 5.00 (s, 2H, CH_2), 6.87–6.90 (m, 4H, Ar-*H*), 6.98 (m, 1H, Ar-*H*), 7.13 (m, 1H, Ar-*H*), 7.20–7.48 (m, 8H, Ar-*H*), 7.82 (s, 2H, Ar-*H*), 9.25 (t, $J = 4.0$ Hz, 1H, CON*H*), 9.54 (t, $J = 4.0$ Hz, 1H, CON*H*) ppm; ^{13}C NMR (100 MHz, DMSO-d_6): δ 45.5 (1C), 46.7 (1C), 55.0 (1C), 119.5 (1C), 119.6 (2C), 119.7 (1C), 119.8 (2C), 125.7 (1C), 131.0 (1C), 133.6 (1C), 133.7 (1C), 133.9 (2C), 134.0 (2C), 134.6 (2C), 135.1 (1C), 139.0 (1C), 139.9 (1C), 140.5 (1C), 140.6 (1C), 145.1 (1C), 152.2 (1C), 164.8 (1C), 167.0 (1C), 167.9 (1C), 170.1 (1C), 170.2 (1C) ppm; IR (KBr): 3279, 3078, 2924, 2855, 1674, 1543, 1512, 1435, 1204 cm^{-1}.

*General procedure for the synthesis of the targeted compounds (**8f–j**)*

The intermediate methyl 3-(3,5-bis(trifluoromethyl)benzyl)-benzylamino)benzoate (**5b**) was dissolved in 1 M sodium hydroxide (5 mL) and refluxed overnight at 100°C, then the reaction mixture was neutralized with 1 M hydrochloric acid and extracted three times using chloroform (3 × 20 mL). The organic layer was dried using anhydrous sodium sulfate and evaporated. Subsequently, the intermediate 3-(3,5-bis-(trifluoromethyl)benzylamino)benzoic acid (**6b**, 0.36 g, 1.0 mmol) was dissolved in 10 mL dichloromethane and oxalyl chloride (**2**, 0.17 mL, 2.0 mmol) was added. The reaction was left under stirring for 5 days at 50–60°C. Later the reaction mixture was evaporated.

*3-{(3,5-Bis(trifluoromethylbenzyl)-[3-(3,5-bis-trifluoromethylbenzylamino)benzoyl]amino}-N-(4-methoxybenzyl)benzamide (**8f**)*

4-Methoxy benzylamine (**7a**, 0.39 mL, 3.0 mmol) was added together with 5 mL of triethylamine and stirred at room temperature for 5 days. Then the crude product was purified by column chromatography using chloroform/methanol (98:2) as eluent to afford **8f** as transparent semisolid (22%); $R_f = 0.94$ ($CHCl_3$/MeOH, 95:5); ^{1}H NMR (300 MHz, $CDCl_3$): δ 3.79 (s, 6H, 2 × OCH_3), 4.21 (d, $J = 6.0$ Hz, 2H, CH_2), 4.55 (d, $J = 6.0$ Hz, 2H, CH_2), 4.99 (s, 2H, CH_2), 6.28–6.49 (m, 1H, Ar-*H*), 6.82 (d, $J = 9.0$ Hz, 2H, Ar-*H*), 6.85 (d, $J = 9.0$ Hz, 2H, Ar-*H*), 7.02 (d, $J = 6.0$ Hz, 1H, Ar-*H*), 7.10 (d, $J = 9.0$ Hz, 2H, Ar-*H*), 7.18–7.26 (m, 2H, Ar-*H*), 7.33–7.42 (m, 1H, Ar-*H*), 7.57 (s, 1H, Ar-*H*), 7.62–7.67 (m, 2H, Ar-*H*), 7.77 (m, 1H, Ar-*H*), 8.56 (t, $J = 6.0$ Hz, 1H, CON*H*), 8.87 (t, $J = 6.0$ Hz, 1H, CON*H*) ppm; ^{13}C NMR (75 MHz, $CDCl_3$): δ 43.0 (1C), 43.8 (2C), 55.4 (2C), 114.2 (2C), 114.3 (2C), 123.0 (1C), 125.0 (1C), 125.3 (1C), 125.7 (1C), 126.3 (1C), 126.8 (1C), 128.9 (1C), 129.2 (1C), 129.3 (2C), 129.5 (2C), 129.8 (1C), 129.9 (1C), 130.2 (1C), 131.8 (1C), 132.2 (1C),

136.1 (1C), 138.1 (1C), 142.0 (1C), 159.3 (2C), 162.0 (1C), 162.1 (1C), 165.9 (1C) ppm; IR (KBr): 3511, 3071, 2924, 2845, 1660, 1582, 1512, 1443, 1381, 1250 cm^{-1}.

*3-{(3,5-Bis(trifluoromethylbenzyl)-[3-(3,5-bis-trifluoromethylbenzylamino)benzoyl]amino}-N-(4-methylbenzyl)benzamide (**8g**)*

4-Methyl benzylamine (**7b**, 0.38 mL, 3.0 mmol) was added together with 5 mL of triethylamine and stirred at room temperature for 5 days. Then the crude product was purified by column chromatography using chloroform/methanol (98:2) as eluent to afford **8g** as transparent semisolid (39%); $R_f = 0.63$ (cyclohexane/ethyl acetate, 60:40); ^{1}H NMR (500 MHz, DMSO-d_6): δ 2.28 (s, 6H, 2 × CH_3), 4.12 (d, $J = 5.25$ Hz, 2H, CH_2), 4.43 (d, $J = 5.50$ Hz, 2H, CH_2), 5.03 (s, 2H, CH_2), 6.78 (d, $J = 7.35$ Hz, 2H, Ar-*H*), 6.97 (d, $J = 7.35$ Hz, 2H, Ar-*H*), 7.14 (d, $J = 7.35$ Hz, 2H, Ar-*H*), 7.21–7.25 (m, 3H, Ar-*H*), 7.29–7.31 (m, 2H, Ar-*H*), 7.33–7.38 (m, 2H, Ar-*H*), 7.90 (d, $J = 7.30$ Hz, 2H, Ar-*H*), 9.03 (t, $J = 5.3$ Hz, 1H, CON*H*), 9.19 (t, $J = 5.5$ Hz, 1H, CON*H*) ppm; ^{13}C-NMR (125 MHz, DMSO-d_6): δ 21.1 (2C), 41.8 (1C), 42.9 (1C), 50.7 (1C), 119.5 (1C), 121.5 (2C), 121.9 (1C), 126.9 (1C), 127.2 (1C), 127.7 (3C), 128.6 (1C), 129.1 (1C), 129.3 (3C), 129.6 (1C), 130.3 (2C), 133.8 (1C), 135.5 (1C), 136.2 (2C), 136.4 (1C), 137.0 (2C), 143.1 (1C), 148.0 (1C), 163.4 (1C), 165.5 (1C), 165.6 (1C) ppm; IR (KBr): 3279, 3032, 2932, 2862, 1651, 1512, 1505, 1451, 1381, 1281 cm^{-1}.

*3-{(3,5-Bis(trifluoromethylbenzyl)-[3-(3,5-bis-trifluoromethylbenzylamino)benzoyl]amino}-N-(3-fluorobenzyl)benzamide (**8h**)*

3-Fluorobenzylamine (**7c**, 0.34 mL, 3.0 mmol) was added together with 5 mL of triethylamine and stirred at room temperature for 5 days. Then the crude product was purified by column chromatography using chloroform/acetone (99:1) as eluent to afford **8h** as off-white powder (20.4%); m.p. 166–167°C; $R_f = 0.40$ ($CHCl_3$/acetone, 95:5); ^{1}H NMR (500 MHz, $CDCl_3$): δ 3.56 (s, 2H, CH_2), 4.48 (d, $J = 6.0$ Hz, 4H, 2 × CH_2), 6.97 (d, $J = 8.7$ Hz, 4H, Ar-*H*), 7.05 (d, $J = 7.4$ Hz, 2H, Ar-*H*), 7.24 (s, 2H, Ar-*H*), 7.28–7.30 (m, 4H, Ar-*H*), 7.79–7.86 (m, 3H, Ar-*H*), 8.89 (t, $J = 6.0$ Hz, 1H, CON*H*), 9.15 (t, $J = 6.0$ Hz, 1H, CON*H*) ppm; ^{13}C NMR (125 MHz, $CDCl_3$): δ 29.7 (1C), 43.2 (2C), 114.6 (1C), 114.7 (2C), 114.8 (1C), 114.9 (2C), 123.2 (2C), 123.3 (2C), 126.6 (1C), 127.4 (1C), 128.1 (2C), 129.3 (1C), 130.3 (2C), 130.4 (2C), 139.2 (1C), 139.3 (1C), 142.3 (1C), 143.4 (1C), 148.2 (1C), 159.6 (2C), 162.0 (1C), 163.9 (1C), 165.6 (1C) ppm; IR (KBr): 3325, 3094, 2924, 2855, 1659, 1551, 1466, 1258 cm^{-1}.

*3-{(3,5-Bis(trifluoromethylbenzyl)-[3-(3,5-bis-trifluoromethylbenzylamino)benzoyl]amino}-N-(3-bromobenzyl)benzamide (**8i**)*

3-Bromobenzylamine (**7d**, 0.38 mL, 3.0 mmol) was added together with 5 mL of triethylamine and stirred at room temperature for 5 days. Then the crude product was purified by column chromatography using chloroform/methanol (95:5) as eluent to afford **8i** as light brown liquid (17.1%); $R_f = 0.70$ ($CHCl_3$/MeOH, 95:5); ^{1}H NMR (500 MHz, DMSO-d_6): δ 3.67 (s, 2H, CH_2), 4.30 (d, $J = 6.3$ Hz, 2H, CH_2), 4.51 (d, $J = 6.4$ Hz, 2H, CH_2), 6.44–6.58 (m, 1H, Ar-*H*), 6.59–6.73 (m, 1H, Ar-*H*), 6.85–7.19 (m, 3H, Ar-*H*), 7.20–7.38 (m, 3H, Ar-*H*), 7.39–7.60 (m, 3H, Ar-*H*), 7.89–8.02 (m, 1H, Ar-*H*), 8.10–8.21 (m, 1H, Ar-*H*), 8.32 (s, 2H, Ar-*H*), 8.45 (t, $J = 6.3$ Hz, 1H, CON*H*), 8.55 (t, $J = 6.4$ Hz, 1H, CON*H*) ppm; ^{13}C NMR (125 MHz, DMSO-d_6): δ 42.6 (2C), 48.3 (1C), 121.1 (1C), 122.5 (2C), 123.6 (1C), 124.9 (2C), 126.1 (1C), 126.2 (1C), 126.5 (1C), 129.1 (1C), 129.2 (1C), 129.5 (2C), 130.2 (2C), 130.9 (2C), 131.0 (1C), 134.6 (2C), 138.2 (1C), 139.3 (2C), 141.2 (1C), 144.5 (1C), 148.6 (1C), 160.8 (1C), 161.5 (1C), 165.4 (1C) ppm; IR (KBr): 3418, 3086, 2994, 2878, 1674, 1597, 1566, 1458, 1427, 1281 cm^{-1}.

*3-{(3,5-Bis(trifluoromethylbenzyl)-[3-(3,5-bis-trifluoromethylbenzylamino)benzoyl]amino}-N-(4-fluorobenzyl)benzamide (**8j**)*

4-Fluorobenzylamine (**7e**, 0.34 mL, 3.0 mmol) was added together with 5 mL of triethylamine and stirred at room temperature for 5 days. Then the crude product was purified by column chromatography using cyclohexane/ethyl acetate (60:40) as eluent to afford **8j** as off-white powder (23.2%); m.p. 126–127°C; $R_f = 0.64$ ($CHCl_3$/MeOH, 98:2); ^{1}H NMR (500 MHz, DMSO-d_6): δ 4.13 (d, 2H, CH_2), 4.47 (d, 2H, CH_2), 5.02 (s, 2H, CH_2), 6.90–7.00 (m, 4H, Ar-*H*), 7.09–7.20 (m, 3H, Ar-*H*), 7.31–7.37 (m, 6H, Ar-*H*), 7.85 (s, 2H, Ar-*H*), 9.09 (t, $J = 4.1$ Hz, 1H, CON*H*), 9.25 (t, $J = 4.2$ Hz, 1H, CON*H*) ppm; ^{13}C NMR (125 MHz, DMSO-d_6): δ 43.1 (1C), 43.3 (1C), 45.2 (1C), 115.2 (1C), 115.3 (1C), 115.4 (1C), 115.5 (2C), 119.5 (1C), 121.5 (2C), 126.7 (1C), 127.8 (1C), 129.3 (1C), 129.4 (1C), 129.5 (1C), 129.6 (1C), 129.7 (1C), 130.3 (2C), 130.7 (1C), 134.7 (1C), 135.7 (1C), 136.1 (1C), 136.4 (1C), 140.9 (1C), 148.0 (1C), 160.7 (1C), 162.6 (1C), 163.4 (1C), 165.4 (1C), 165.5 (1C) ppm; IR (KBr): 3441, 3081, 2940, 1651, 1506, 1474, 1397 cm^{-1}.

Computational methods

Preparation of protein structures

The X-ray crystal structure of CETP (PDB ID: 4EWS) [30] was adopted from the RCSB Protein Data Bank. CETP structure was prepared and energetically minimized using the Protein Preparation [28] panel in the Schrödinger software enterprise to maximize H-bond interactions.

Preparation of ligand structures

The synthesized compounds (ligands) were built based on the co-crystallized ligand's (ORP) coordinates in 4EWS [30]. The ligands were built using MAESTRO build wizard and energetically minimized by MacroModel [28] program recruiting the OPLS2005 force field.

Glide docking

The Grid file for CETP was generated employing the Glide Grid Generation [28] procedure with the bound ligand as centroid. During the docking process, the scaling factor for van der Waals for the nonpolar atoms was set to 0.8 to facilitate some flexibility for the protein side chains. All other parameters were set as defaults. The binding affinity was represented in

terms of docking scores (kcal/mol). The more negative the docking score, the better the binder.

Pharmacophore mapping

Utilizing a previously generated pharmacophore model by our group [16], and in order to get further details about the functionalities of the synthesized compounds responsible for activity, **8a–j** were mapped against the adopted pharmacophore model of CETP inhibitors [16].

In vitro CETP inhibition bioassay

An aliquot of rabbit serum (1.5 μL) was mixed with 160 μL of the tested sample. The donor and acceptor molecules in the assay buffer were added, mixed well, and the volume was adjusted to 203 μL using the assay buffer.

Then, the mixture was incubated at 37°C for 1 h. Fluorescence intensity (excitation λ: 465 nm; emission λ: 535 nm) was read using FLX800TBI microplate fluorimeter (BioTek Instruments, Winooski, VT, USA).

The synthesized molecules were dissolved in DMSO yielding 10 mM stock solutions. Next, dilution to the required concentration was attained using distilled deionized water. DMSO concentration was adjusted to 0.1%. CETP activity is not affected by DMSO. The percentage of residual CETP activity was identified in the presence and absence of the tested molecules.

Negative control samples missing rabbit serum were used as a contrast background. Torcetrapib was used as a standard CETP inhibitor. The experimental protocol and measurements were carried out in duplicates [23].

$$\%\text{Inhibition} = [1 - (\text{Inhibitor}_{\text{read}} - \text{Blank}_{\text{read}})/$$

$$(\text{Positive control} - \text{Negative control})] \times 100\%$$

The authors acknowledge the Scientific Research and Postgraduate Deanship at Al-Zaytoonah University of Jordan for sponsoring this project.

The authors have declared no conflict of interest.

References

[1] M. Nichols, N. Townsend, P. Scarborough, M. Rayner, *Eur. Heart J*. **2014**, *35*(42), 2950–2959.
[2] A. K. Shrivastava, H. V. Singh, A. Raizada, S. K. Singh, *EHJ* **2015**, *67*(2), 89–97.
[3] A. N. Orekhov, E. A. Ivanova, *Phytomedicine* **2016**, *23*(11), 1190–1197.
[4] C. E. Kosmas, E. DeJesus, D. Rosario, T. J. Vittorio, *Clin. Med. Insights Cardiol*. **2016**, *10*, 37–42.
[5] R. Abu Khalaf, G. Abu Sheikha, M. Al-Sha'er, G. Albadawi, M. Taha, *Med. Chem. Res*. **2012**, *21*, 3669–3680.
[6] M. Ayaori, *Rinsho Byori*. **2016**, *64*(1), 57–65.
[7] C. G. Santos-Gallego, J. J. Badimon, R. S. Rosenson, *Endocrinol. Metab. Clin. North Am*. **2014**, *43*(4), 913–947.
[8] T. Aghebati, A. Badiee, A. H. Mohammadpour, M. Afshar, M. R. Jaafari, K. Abnous, S. Issazadeh, S. Hashemzadeh, M. Zareh, H. Hashemizadeh, S. Nazemi, *Biomed. Pharmacother*. **2016**, *81*, 468–473.
[9] H. L. Xie, C. C. Liu, Y. Q. Li, C. L. Bai, C. Z. Hao, J. Guo, C. Q. Luo, D. M. Zhao, M. S. Cheng, *jcclet*. **2017**, *28*(2), 260–263.
[10] D. Zhao, H. Xie, C. Bai, C. Liu, C. Hao, S. Zhao, H. Yuan, C. Luo, J. Wang, B. Lin, J. Zheng, M. Cheng, *Bioorg. Med. Chem*. **2016**, *24*(8), 1589–1597.
[11] G. Abu Sheikha, R. Abu Khalaf, A. Melhem, G. Albadawi, *Molecules* **2010**, *15*, 5721–5733.
[12] H. Xie, Y. Li, C. Bai, R. Wang, C. Liu, C. Hao, B. Lin, M. Cheng, D. Zhao, *Bioorg. Med. Chem*. **2016**, *24*(8), 1811–1818.
[13] B. Simic, P. Mocharla, M. Crucet, E. Osto, A. Kratzer, S. Stivala, S. Kühnast, T. Speer, P. Doycheva, H. M. Princen, J. W. van der Hoorn, J. W. Jukema, H. Giral, A. Tailleux, U. Landmesser, B. Staels, T. F. Lüscher, *Atherosclerosis* **2017**, *257*, 186–194.
[14] D. Pirim, X. Wang, V. Niemsiri, Z. H. Radwan, C. H. Bunker, J. E. Hokanson, R. F. Hamman, M. M. Barmada, F. Y. Demirci, M. I. Kamboh, *Metabolism* **2016**, *65*(1), 36–47.
[15] Y. Chang, S. Zhou, E. Li, W. Zhao, Y. Ji, X. Wen, H. Sun, H. Yuan, *Eur. J. Med. Chem*. **2017**, *126*, 143–153.
[16] R. Abu Khalaf, S. Al-Rawashdeh, D. Sabbah, G. Abu Sheikha, *Med. Chem*. **2017**, *13*(3), 239–253.
[17] V. García-González, B. Delgado-Coello, A. Pérez-Torres, J. Mas-Oliva, *J. Arch. Med. Res*. **2015**, *46*(5), 427–437.
[18] M. Hoekstra, *Atherosclerosis* **2017**, *01*, 034.
[19] P. J. Barter, K. A. Rye, R. M. Touyz, *Pharmacol. Rev*. **2016**, *68*(2), 458–475.
[20] M. M. Page, A. J. Hooper, J. R. Burnett, *Expert Opin. Pharmacother*. **2016**, *17*(2), 275–281.
[21] J. Girona, D. Ibarretxe, N. Plana, S. Guaita-Esteruelas, N. Amigo, M. Heras, L. Masana, *Cardiovasc. Diabetol*. **2016**, *15*(1), 107.
[22] X. M. Bu, D. M. Niu, J. Wu, Y. L. Yuan, J. X. Song, J. J. Wang, *Lipids Health Dis*. **2017**, *16*, 4.
[23] R. Abu Khalaf, G. Abu Sheikha, Y. Bustanji, M. O. Taha, *Eur. J. Med. Chem*. **2010**, *45*, 1598–1617.
[24] M. Zhang, R. Charles, H. Tong, L. Zhang, M. Patel, F. Wang, M. J. Rames, A. Ren, K. A. Rye, X. Qiu, D. G. Johns, M. A. Charles, G. Ren, *Sci. Rep*. **2015**, *5*, 8741.
[25] R. Abu Khalaf, H. Abd El-Aziz, D. Sabbah, G. Albadawi, G. Abu Sheikha, *Lett. Drug Des. Discov*. **2017**, *14*, 1391.
[26] R. A. Friesner, J. L. Banks, R. B. Murphy, T. A. Halgren, J. J. Klicic, D. T. Mainz, M. P. Repasky, E. H. Knoll, M. Shelley, J. K. Perry, D. E. Shaw, P. Francis, P. S. Shenkin, *J. Med. Chem*. **2004**, *47*, 1739–1749.

[27] R. A. Friesner, R. B. Murphy, M. P. Repasky, L. L. Frye, J. R. Greenwood, T. A. Halgren, P. C. Sanschagrin, D. T. Mainz, *J. Med. Chem*. **2006**, *49*, 6177–6196.
[28] Prote in Preparation Wizard, Maestro, Macromodel, and QPLD-dock, Schrödinger, LLC, Portland, OR, U.S.A. 97204, **2016**.
[29] The Molecular Operating Environment Chemical Computing Group, Inc Montreal, Quebec, Canada, **2016**.
[30] S. Liu, A. Mistry, J. M. Reynolds, D. B. Lloyd, M. C. Griffor, D. A. Perry, R. B. Ruggeri, R. W. Clark, X. Qiu, *J. Biol. Chem*. **2012**, *287*, 37321–37329.